ELSEVIER

Journal of Biomechanics 40 (2007) 543–553

JOURNAL OF BIOMECHANICS

www.elsevier.com/locate/jbiomech
www.JBiomech.com

Adjustments to McConville et al. and Young et al. body segment inertial parameters

R. Dumas*, L. Chèze, J.-P. Verriest

Laboratoire de Biomécanique et Modélisation Humaine, Université Claude Bernard Lyon 1 – INRETS, Bâtiment Omega, 43 Boulevard du 11 novembre 1918, 69 622 Villeurbanne cedex, France

Accepted 21 February 2006

Abstract

Body segment inertial parameters (BSIPs) are important data in biomechanics. They are usually estimated from predictive equations reported in the literature. However, most of the predictive equations are ambiguously applicable in the conventional 3D segment coordinate systems (SCSs). Also, the predictive equations reported in the literature all include two assumptions: the centre of mass and the proximal and distal endpoints are assumed to be aligned, and the inertia tensor is assumed to be principal in the segment axes. These predictive equations, restraining both position of the centre of mass and orientation of the principal axes of inertia, become restrictive when computing 3D inverse dynamics, when analyzing the influence of BSIP estimations on joint forces and moments and when evaluating personalized 3D BSIPs obtained from medical imaging.

In the current study, the extensive data from McConville et al. (1980. Anthropometric relationships of body and body segment moments of inertia. AFAMRL-TR-80-119, Aerospace Medical Research Laboratory, Wright–Patterson Air Force Base, Dayton, Ohio) and from Young et al. (1983. Anthropometric and mass distribution characteristics of the adults female. Technical Report AFAMRL-TR-80-119, FAA Civil Aeromedical Institute, Oklaoma City, Oklaoma) are adjusted in order to correspond to joint centres and to conventional segment axes. In this way, scaling equations are obtained for both males and females that provide BSIPs which are directly applicable in the conventional SCSs and do not restrain the position of the centre of mass and the orientation of the principal axes. These adjusted scaling equations may be useful for researchers who wish to use appropriate 3D BSIPs for posture and movement analysis.

Keywords: Body segment inertial parameters; Adjustment; Scaling equations; Joint centres; Segment coordinate system

1. Introduction

Body segment inertial parameters (BSIPs) are important data for the biomechanical analysis of human movement and posture in sports, ergonomics, rehabilitation and orthopaedics (Jensen, 1993; Pearsall and Reid, 1994; Reid and Jensen, 1990). BSIPs are usually estimated from predictive equations reported in the literature (Ackland et al., 1988a; Clauser et al., 1969; de Leva, 1996; Dempster, 1955; Durkin and Dowling, 2003; Hinrichs, 1985; Hinrichs, 1990; Jensen, 1978, 1986; McConville et al., 1980; Pavol et al., 2002; Schneider and Zernicke, 1992; Yeadon and Morlock, 1989; Young et al., 1983; Zatsiorsky and Seluyanov, 1983) using linear or non-linear regressions. The predictive equations are limited by the measurement techniques (e.g. uniform densities) and moreover by the population on which they are based (e.g. small sample, elder males, …). Therefore, the predictive equations should not be used outside the population on which they are based

*Corresponding author. Tel.: +33 4 72 44 85 75; fax: +33 4 72 44 80 54.
E-mail address: raphael.dumas@univ-lyon1.fr (R. Dumas).

0021-9290/$ - see front matter © 2006 Elsevier Ltd. All rights reserved.
doi:10.1016/j.jbiomech.2006.02.013

(Pearsall and Reid, 1994; Reid and Jensen, 1990). Instead, non-linear regressions (Yeadon and Morlock, 1989; Zatsiorsky and Seluyanov, 1983) should be preferred. However, linear regressions such as scaling equations, based on total body mass and segment length, are more commonly used because of their expediency. For instance, for young adults, the scaling equations of de Leva (1996) represent the most complete and practical series of predictive equations, making a distinction between genders, and providing all frontal, sagittal and horizontal moments of inertia. The original data from Zatziorsky and Seluyanov (1983) have been adjusted by de Leva (1996) in order to consider segment lengths based on joint centres instead of anatomical landmarks.

Although convenient, the predictive equations refer to frontal, sagittal and horizontal planes of the segments, sometimes not clearly defined, and it is therefore ambiguous how to apply 3D BSIPs in the conventional segment coordinate systems (SCSs) (Cappozzo et al., 1995, Wu et al., 2002, 2005). Furthermore, in all the predictive equations reported in the literature, two assumptions are considered: (1) the centre of mass and the proximal and distal endpoints are assumed to be aligned, and (2) the inertia tensor is assumed to be principal in the axes of the segment. These predictive equations, being ambiguously applicable in the SCSs and restraining both position of the centre of mass and orientation of the principal axes of inertia, become restrictive when computing 3D inverse dynamics (Apkarian et al., 1989; Davis et al., 1991; Doriot and Chèze, 2004; Dumas et al., 2004; Kadaba et al., 1989; Vaughan et al., 1992). These predictive equations also have limitations when analyzing the influence of BSIP estimations on joint forces and moments as all published studies (Andrews and Mish, 1996; Kingma et al., 1996; Krabbe et al., 1997; Pearsall and Costigan, 1999; Rao et al., 2005) still consider both assumptions. This is also the case when evaluating BSIPs obtained from medical imaging as all the personalized 3D BSIPs (Cheng et al., 2000; Dumas et al., 2005; Durkin et al., 2002; Ganley and Powers, 2004; Mungiole and Martin, 1990; Pearsall et al., 1996, 1994) can only be compared to plane by plane and restrictive estimations. Therefore, there is a lack of predictive equations in the literature providing appropriate 3D BSIPs: that is to say BSIPs directly applicable in the conventional SCSs and without restrictive assumptions.

The data of McConville et al. (1980) and of Young et al. (1983) are among the few published extensive BSIPs. For 30 years old males and females, these studies provide the 3D locations of the segment centres of mass, the principal moments of inertia and the orientations of the principal axes of inertia with respect to anatomical axes. However, the anatomical axes (based on anatomical landmarks) differ from the segment axes used in the conventional SCSs (Cappozzo et al., 1995; Wu et al., 2002, 2005). These data have been used for the definition of dummy specifications (Schneider et al., 1983) but are not widely used for movement and posture analysis.

The objective of this paper is to adjust the data of McConville et al. (1980) and of Young et al. (1983) in order to: (1) express BSIPs directly in the conventional SCSs and (2) establish scaling equations without restraining the position of the centre of mass and the orientation of the principal axes of inertia.

2. Adjustment procedure and results

2.1. Original data

McConville et al. (1980) studied 31 adult males (mean age 27.5 years old, mean weight 80.5 kg, mean stature 1.77 m). Young et al. (1983) studied 46 females (mean age 31.2 years old, mean weight 63.9 kg, mean stature 1.61 m). Both populations were chosen to represent the entire stature/weight distribution. Both studies were performed on living subjects using the same stereo-photogrammetric technique. This technique allows the computation of segment volumes through the 3D reconstruction of surface points. Some of the points were anatomical landmarks. Other points were placed every 7 mm on horizontal cross sections. The interval between cross sections was 25 mm (or 13 mm for the *Head*, *Hands*, *Feet* and *Abdomen*). The BSIPs were then computed assuming a uniform density of $1\,g.cm^{-2}$. Both studies used the same segmentation, the 17 segments being the *Head*, *Neck*, *Thorax*, *Abdomen*, *Pelvis*, right and left *Arms*, *Forearms*, *Hands*, *Thighs*, *Legs* and *Feet*. For every segment, a set of anatomical landmarks were provided in an anatomical coordinates system (ACS), following the same definition in both studies. The reported BSIPs were the segment mass, the principal moments of inertia, the 3D location of the centre of mass and the orientation of the principal axes of inertia with respect to the ACS. Additionally, both studies provide anthropometric measurements.

This stereo-photogrammetric technique was reported to provide the position of centre of mass with an averaged error of 5.6% when compared to direct measurements from six cadavers (McConville and Clauser, 1976). For the frontal, sagittal and horizontal principal moments of inertia, the average errors were of 3.5%, 3.9%, and 5.8%, respectively. For the segment mass, the average errors were under 5% for the *Head*, *Forearms*, *Legs* and *Feet* and remained under 10% for the *Trunk* (standing for *Neck* plus *Thorax* plus *Abdomen* plus *Pelvis*), *Arms*, *Thighs* and *Hands*.

2.2. Transformation from one anatomical coordinate system to another

In the adjustment procedure, the segment lengths and the SCSs are based on the joint centres. Using selected anatomical landmarks, each joint centre can be estimated in one ACS. The transformation from one ACS to another is required in order to obtain the position of the joint centre in both adjacent segments.

Young et al. (1983) provided at least three anatomical landmarks expressed at the same time in two adjacent ACSs. This allows the computation of the transformation (i.e. rotation and translation) from one ACS to the other by singular value decomposition (Soderkvist and Wedin, 1993).

McConville et al. (1980) provided the 3D location of fewer than three anatomical landmarks at the same time in two adjacent ACSs. However, the rotation from one ACS to the other is assumed to be the same as for Young et al. (1983) and the translation is deduced from at least one anatomical landmark expressed at the same time in both ACSs.

2.3. Joint centres and segment coordinate systems

Based on selected anatomical landmarks (Fig. 1, Appendix A), the joint centres are estimated and the SCSs are constructed according to the literature (Cappozzo et al., 1995; Rao et al., 1996; Wu et al., 2002, 2005). The adjustment procedure concerns nine segments: *Head & Neck*, *Torso*, *Pelvis*, *Arm*, *Forearm*, *Hand*, *Thigh*, *Leg* and *Foot*. Symmetry is assumed between the right and left limbs. A single segment, *Torso*, standing for *Thorax* plus *Abdomen* is considered because, in the adjustment procedure, no applicable joint centre estimation was available for the *Thoracic Joint Centre*.

2.3.1. Pelvis

The *Right* and *Left Antero-Superior Iliac Spines* (*RASIS* and *LASIS*) and the *Symphision* (*SYM*) are available in the *Pelvis* ACS. This allows the estimation of the *Lumbar Joint Centre* (*LJC*) and the *Hip Joint Centre* (*HJC*) according to Reed et al. (1999). For details see Appendix B.

The *Z*-axis of the *Pelvis* SCS runs from the *LASIS* to the *RASIS*. The *Y*-axis is normal to a plane containing the *LASIS*, the *RASIS* and the *Midpoint between the Postero-Superior Iliac Spines* (*MPSIS*), pointing cranially. The *X*-axis is the cross product of the *Y* and *Z* axes. The origin is the *LJC*.

2.3.2. Torso

The 7th *Cervicale* (C_7), the *Suprasternale* (*SUP*) and the *Right* and *Left Acromion* (*RA* and *LA*) are available in the *Thorax* ACS. This allows the estimation of the *Cervical Joint Centre* (*CJC*) and the *Shoulder Joint*

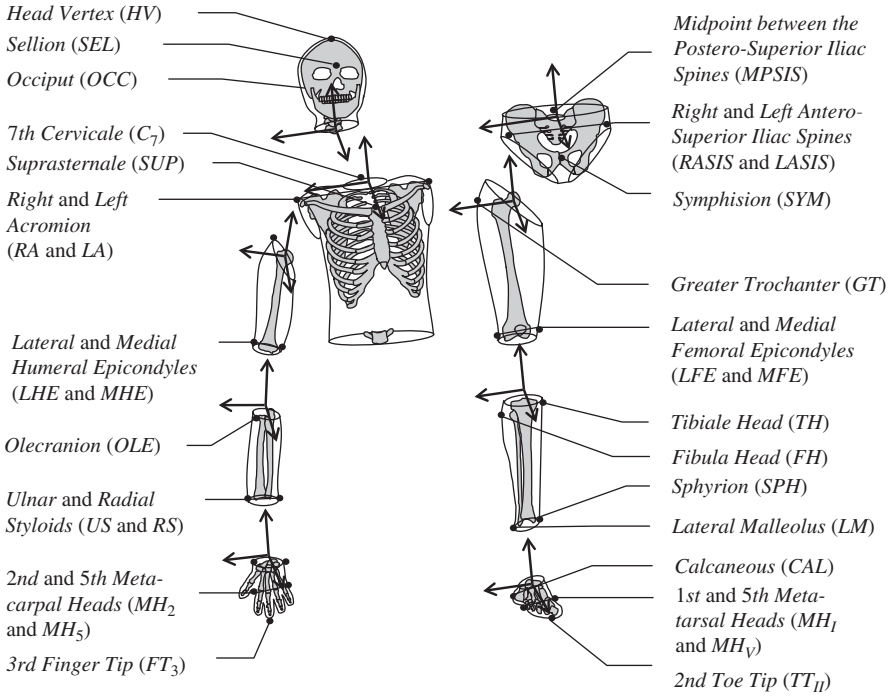

Fig. 1. Locations of selected anatomical landmarks from McConville et al. (1980) and from Young et al. (1983) and orientations of the segment coordinate system (SCSs) built from these landmarks.

Centre (*SJC*) according to Reed et al. (1999). For details see Appendix C.

The *LJC* is then transformed from the *Pelvis* ACS into the *Thorax* ACS. The *Y*-axis of the *Torso* SCS runs from the *LJC* to the *CJC*. The *Z*-axis is normal to a plane containing the *LJC*, *CJC*, and *SUP*, pointing laterally. The *X*-axis is the cross product of the *Y*- and *Z*-axes. The origin is the *CJC*.

2.3.3. Head & Neck

The *CJC* is transformed from the *Thorax* ACS into the *Head* ACS. The *Y*-axis of the *Head & Neck* SCS runs from the *CJC* to the *Head Vertex* (*HV*). The *Z*-axis is normal to a plane containing the *HV*, the *CJC*, and the *Sellion* (*SEL*), pointing laterally. The *X*-axis is the cross product of the *Y*- and *Z*-axes. The origin is the *CJC*.

2.3.4. Arm

The *Lateral* and *Medial Humeral Epicondyles* (*LHE* and *MHE*) are available in the *Arm* ACS. The *Elbow Joint Centre* (*KJC*) is estimated as the midpoint between the *LHE* and *MHE*.

The *SJC* is then transformed from the *Thorax* ACS into the *Arm* ACS. The *Y*-axis of the *Arm* SCS runs from the *EJC* to the *SJC*. The *X*-axis is normal to a plane containing the *SJC*, *LHE* and *MHE*, pointing anteriorly. The *Z*-axis is the cross product of the *X*- and *Y*-axes. The origin is the *SJC*.

2.3.5. Forearm

The *Ulnar* and *Radial Styloids* (*US* and *RS*) are available in the *Forearm* ACS. The *Wrist Joint Centre* (*WJC*) is estimated as the midpoint between the *US* and *RS*.

The *EJC* is then transformed from the *Arm* ACS into the *Forearm* ACS. The *Y*-axis of the *Forearm* SCS runs from the *WJC* to the *EJC*. The *X*-axis is normal to a plane containing the *EJC*, *US* and *RS*, pointing anteriorly. The *Z*-axis is the cross product of the *X*- and *Y*-axes. The origin is the *EJC*.

2.3.6. Hand

The *US* and *RS* (and thus the *WJC*) are also available in the *Hand* ACS. The *Y*-axis of the *Hand* SCS runs from the midpoint between the 2nd and 5th *Metacarpal Heads* (MH_2 and MH_5) to the *WJC*. The *X*-axis is normal to a plane containing the *WJC*, MH_2 and MH_5, pointing anteriorly. The *Z*-axis is the cross product of the *X*- and *Y*-axes. The origin is the *WJC*.

2.3.7. Thigh

The *Lateral* and *Medial Femoral Epicondyles* (*LFE* and *MFE*) are available in the *Thigh* ACS. The *Knee Joint Centre* (*KJC*) is estimated as the midpoint between the *LFE* and *MFE*.

The *HJC* is then transformed from the *Pelvis* ACS into the *Thigh* ACS. The *Y*-axis of the *Thigh* SCS runs from the *KJC* to the *HJC*. The *X*-axis is normal to a plane containing the *HJC*, *LFE* and *MFE*, pointing anteriorly. The *Z*-axis is the cross product of the *X*- and *Y*-axes. The origin is the *HJC*.

2.3.8. Leg

The *Lateral Malleolus* (*LM*) and the *Sphyrion* (*SPH*) are available in the *Leg* ACS. The *Ankle Joint Centre* (*AJC*) is estimated as the midpoint between the *LM* and *SPH*.

The *KJC* is then transformed from the *Thigh* ACS into the *Leg* ACS. The *Y*-axis of the *Leg* SCS runs from the *AJC* to the *KJC*. The *X*-axis is normal to a plane containing the *KJC*, the *AJC* and the *Fibula Head* (*FH*), pointing anteriorly. The *Z*-axis is the cross product of the *X*- and *Y*-axes. The origin is the *KJC*.

2.3.9. Foot

The *AJC* is transformed from the *Leg* ACS into the *Foot* ACS. The *X*-axis of the *Foot* SCS runs from the *Calcaneous* (*CAL*) to the midpoint between the 1st and 5th *Metatarsal Heads* (MH_I and MH_V). The *Y*-axis is normal to a plane containing the *CAL*, MH_I and MH_V, pointing cranially. The *Z*-axis is the cross product of the *X*- and *Y*-axes. The origin is the *AJC*.

2.4. Segment length

For the *Arm*, *Forearm*, *Thigh* and *Leg*, the segment length *L* is computed as the distance between the proximal and the distal joint centres. For the *Head & Neck*, the segment length is the distance between the *CJC* and the *HV*. For the *Hand*, the segment length is the distance between the *WJC* and the midpoint between the MH_2 and MH_5. An alternative segment length is between the *WJC* and the 3rd *Finger Tip* (FT_3). For the *Foot*, the segment length is the distance between the *AJC* and the midpoint between the MH_I and MH_V. An alternative segment length is between the *CAL* and the 2nd *Toe Tip* (TT_II). For the *Pelvis*, the segment length is the distance between the *LJC* and the projection of the *HJC* in sagittal plane. An alternative segment length is the *Pelvis Width* (i.e. the distance between the *RASIS* and the *LASIS*). For the *Torso*, the segment length is the distance between the *CJC* and the *LJC*. An alternative segment length is the *Thorax Width* (i.e. the distance between the C_7 and the *SUP*).

2.5. Adjusted body segment inertial parameters and scaling equations

For every segment, the selected anatomical landmarks (Fig. 1), including the centre of mass are adjusted with the transformation from the ACS into the SCS. The

Table 1
(A) Adjusted 3D positions of the anatomical landmarks and the centres of mass in the segment coordinate systems (SCSs) of the upper body. (B) Adjusted 3D positions of the anatomical landmarks and the centres of mass in the segment coordinate systems (SCSs) of the lower body—see Section 2.3 in the text for the SCS definitions

		Female			Male		
Segment	Anatomical landmark	X (in mm)	Y (in mm)	Z (in mm)	X (in mm)	Y (in mm)	Z (in mm)
A. Upper body							
Head & Neck	*Head Vertex (HV)*	0	221	0	0	244	0
	Sellion (SEL)	79	127	0	83	137	0
	Occiput (OCC)	−99	95	0	−107	103	0
	Centre Of Mass (COM)	−15	132	0	−15	136	0
Torso	*7th Cervicale (C_7)*	−57	34	0	−69	34	0
	Suprasternale (SUP)	45	−39	0	46	−45	0
	Right Acromion (RA)	−30	−22	181	−21	−31	209
	Shoulder Joint Centre (SJC)	13	−73	181	21	−73	209
	Lumbar Joint Centre (LJC)	0	−427	0	0	−478	0
	Centre Of Mass (COM)	−7	−186	−2	−17	−201	−1
Arm	*Right Acromion (RA)*	−35	56	4	−25	54	3
	Lateral Humeral Epicondyle (LHE)	0	−221	34	0	−258	41
	Medial Humeral Epicondyle (MHE)	0	−238	−34	0	−264	−41
	Centre Of Mass (COM)	−16	−104	−6	5	−118	−7
Forearm	*Olecranion (OLE)*	−12	8	−19	−8	14	−22
	Ulnar Styloid (US)	0	−242	−27	0	−284	−33
	Radial Styloid (RS)	0	−252	27	0	−284	33
	Centre Of Mass (COM)	5	−102	5	3	−118	4
Hand	*Ulnar Styloid (US)*	−11	−1	−25	−7	0	−32
	Radial Styloid (RS)	11	1	25	7	0	32
	2nd Metacarpal Head (MH_2)	0	−79	38	0	−86	46
	5th Metacarpal Head (MH_5)	0	−63	−38	0	−75	−46
	3rd Finger Tip (FT_3)	14	−166	−13	7	−189	1
	Centre Of Mass (COM)	5	−55	3	7	−68	6
B. Lower body							
Pelvis	*Midpoint between the Postero-Superior Iliac Spines (MPSIS)*	−108	−13	0	−102	7	0
	Right Antero-Superior Iliac Spine (RASIS)	87	−13	119	78	7	112
	Left Antero-Superior Iliac Spine (LASIS)	87	−13	−119	78	7	−112
	Symphision (SYM)	123	−97	0	123	−67	0
	Hip Joint Centre (HJC)	54	−93	88	56	−75	81
	Centre Of Mass (COM)	−1	−25	0	3	−26	0
Thigh	*Greater Trochanter (GT)*	−19	8	87	−40	6	101
	Lateral Femoral Epicondyle (LFE)	0	−375	57	0	−431	57
	Medial Femoral Epicondyle (MFE)	0	−382	−57	0	−432	−57
	Centre Of Mass (COM)	−29	−143	3	−18	−185	14
Leg	*Tibiale Head (TH)*	8	−22	−39	21	−27	−42
	Fibula Head (FH)	0	−40	60	0	−23	47
	Sphyrion (SPH)	10	−387	−31	21	−434	−33
	Lateral Malleolus (LM)	−10	−390	31	−21	−433	33
	Centre Of Mass (COM)	−19	−157	12	−21	−178	3
Foot	*Calcaneous (CAL)*	−59	−46	12	−46	−21	7
	1st Metatarsal Head (MH_I)	116	−46	−33	146	−21	−47
	5th Metatarsal Head (MH_V)	97	−46	57	128	−21	60
	2nd Toe Tip (TT_{II})	174	−54	9	219	−9	−1
	Centre Of Mass (COM)	45	−36	6	45	−36	6

adjusted 3D positions of these selected anatomical landmarks are given in Table 1A and B.

The 3D vectors from the origin to the centre of mass are then expressed relative to the segment length L. For the *Pelvis*, an alternative origin is the midpoint between the *LASIS* and *RASIS*. For the *Torso*, an alternative origin is the *SUP*. For the *Foot*, an alternative origin is the *CAL*. The segment masses m are expressed relative to the total body mass (without adjustment). From the principal moments of inertia, considering the orientation of the principal axes with respect to the anatomical axes and the orientation of the ACS with respect to the

Table 2
Definition of the segment lengths and of the origins of the segment coordinate systems (SCSs)—values of the segment length L (used for scaling) and of the scaling factors for the segment mass m, the position of centre of mass, the moments of inertia and the products of inertia (i denotes negative product of inertia)—see Section 2.5 in the text for an example of the use of this Table

Segment	Length definition	Origin of SCS	Gender	Length L (in mm)	Scaling factor for mass m (%)	Scaling factors for position of centre of mass			Scaling factors for tensor of inertia					
						X (%)	Y (%)	Z (%)	r_{xx} (%)	r_{yy} (%)	r_{zz} (%)	r_{xy} (%)	r_{xz} (%)	r_{yz} (%)
Head & Neck	*CJC* to *HV*	*CJC*	F	221	6.7	−7.0	59.7	0	32	27	34	6(i)	1	1(i)
			M	244	6.7	−6.2	55.5	0.1	31	25	33	9(i)	2(i)	3
Torso	*CJC* to *LJC*	*CJC*	F	429	30.4	−1.6	−43.6	−0.6	29	27	29	22	5	5(i)
			M	477	33.3	−3.6	−42.0	−0.2	27	25	28	18	2	4(i)
Arm	*SJC* to *EJC*	*SJC*	F	243	2.2	−7.3	−45.4	−2.8	33	17	33	3	5(i)	14
			M	271	2.4	1.7	−45.2	−2.6	31	14	32	6	5	2
Forearm	*EJC* to *WJC*	*EJC*	F	247	1.3	2.1	−41.1	1.9	26	14	25	10	4	13(i)
			M	283	1.7	1.0	−41.7	1.4	28	11	27	3	2	8(i)
Hand	*WJC* to midpoint between MH_2 and MH_5	*WJC*	F	71	0.5	7.7	−76.8	4.8	63	43	58	29	23	28(i)
			M	80	0.6	8.2	−83.9	7.4	61	38	56	22	15	20(i)
Pelvis	*LJC* to projection of *HJC* in sagittal plane	*LJC*	F	107	14.6	−0.9	−23.2	0.2	91	100	79	34(i)	1(i)	1(i)
			M	94	14.2	2.8	−28.0	−0.6	101	106	95	25(i)	12(i)	8(i)
Thigh	*HJC* to *KJC*	*HJC*	F	379	14.6	−7.7	−37.7	0.9	31	19	32	7	2(i)	7(i)
			M	432	12.3	−4.1	−42.9	3.3	29	15	30	7	2(i)	7(i)
Leg	*KJC* to *AJC*	*KJC*	F	388	4.5	−4.9	−40.4	3.1	28	10	28	2	1	6
			M	433	4.8	−4.8	−41.0	0.7	28	10	28	4(i)	2(i)	5
Foot	*AJC* to midpoint between MH_I and MH_V	*AJC*	F	165	1.0	27.0	−21.8	3.9	17	36	35	10(i)	6	4(i)
			M	183	1.2	38.2	−15.1	2.6	17	37	36	13	8(i)	0
Alternative length and origin														
Torso	C_7 to *SUP*	*SUP*	F	125	30.4	−41.1	−117.3	−1.9	98	93	98	76	16	19(i)
			M	139	33.3	−45.6	−112.1	−0.8	93	85	96	62	7	13(i)
Hand	*WJC* to FT_3	*WJC*	F	167	0.5	3.3	−32.7	2.1	27	18	25	12	10	12(i)
			M	189	0.6	3.5	−35.7	3.2	26	16	24	9	7	8(i)
Pelvis	Midpoint between *RASIS* to *LASIS*	Middle of *RASIS* and *LASIS*	F	238	14.6	−37.1	−5.0	0.1	41	45	36	15(i)	0	0
			M	224	14.2	−33.6	−14.9	−0.3	42	44	40	10(i)	5(i)	3(i)
Foot	*CAL* to TT_{II}	*CAL*	F	233	1.0	44.3	4.4	−2.5	12	25	25	7(i)	5	3(i)
			M	265	1.2	43.6	−2.5	−0.7	11	25	25	9	6(i)	0

SCS, the inertia tensor is calculated in the segment axes. Both products and moments of inertia I_{ij} are expressed relative to the segment length L and the segment mass m with the following relation: $r_{ij} = (1/L)\sqrt{I_{ij}/m}$.

For the moments of inertia (I_{ij}, $i = j$), r_{ij} corresponds to the relative radius of gyration. The same scaling equation is also used for the products of inertia (I_{ij}, $i \neq j$), but does not represent radii of gyration (r_{ij} may be imaginary value when products are negative). For the *Head & Neck*, the adjusted segment mass, centre of mass, moments and products of inertia are obtained by combining *Head* plus *Neck*. For the *Torso*, the adjusted segment mass, centre of mass, moments and products of inertia are obtained by combining *Thorax* plus *Abdomen*.

The adjusted BSIP scaling equations are given in Table 2 (alternative origins and/or segment lengths for the *Torso*, *Hand*, *Pelvis* and *Foot* are also provided). Notation (i) indicates that the product of inertia is negative. This could be directly taken into account if considering a complex number. For example, concerning the *Thigh* of a young man (of weight m_{Body}), the scaling equations can be used as follows. The *Thigh* length L_{Thigh} (from the *HJC* to the *KJC*), can be obtained during 3D gait analysis, at the same time as the *Thigh* SCS is constructed (Wu et al., 2002). In this SCS (with the origin at the *HJC*), the 3D position of centre of mass and the complete inertia tensor are directly

$$\begin{bmatrix} -0.041L_{\mathrm{Thigh}} \\ -0.429L_{\mathrm{Thigh}} \\ 0.033L_{\mathrm{Thigh}} \end{bmatrix} \text{ and}$$

$$\begin{bmatrix} (0.29L_{\mathrm{Thigh}})^2 & (0.07L_{\mathrm{Thigh}})^2 & (0.02iL_{\mathrm{Thigh}})^2 \\ (0.07L_{\mathrm{Thigh}})^2 & (0.15L_{\mathrm{Thigh}})^2 & (0.07iL_{\mathrm{Thigh}})^2 \\ (0.02iL_{\mathrm{Thigh}})^2 & (0.07iL_{\mathrm{Thigh}})^2 & (0.30L_{\mathrm{Thigh}})^2 \end{bmatrix} \times 0.123m_{\mathrm{Body}},$$

where $0.123 \times m_{\mathrm{Body}}$ is the mass of the *Thigh* segment.

As the scaling equations for the products of inertia do not represent real physical quantities, the principal moments of inertia and the orientation of the principal axes of inertia with respect to the SCS were also computed. The principal radii of gyration and the nine elements of the rotation matrix (principal axes of inertia with respect to the SCS) are given for each segment in Appendix D.

3. Discussion

The biomechanical modelling of the human body for posture and movement analysis is classically based on a system of linked segments (Chaffin and Anderson, 1991). Therefore, the segment endpoints logically correspond to proximal and distal joint centres. However, when BSIPs are considered, several predictive equations propose other segment endpoint definitions (Clauser et al., 1969; McConville et al., 1980; Young et al., 1983; Zatsiorsky and Seluyanov, 1983) which are less appropriate. As a result, adjustment procedures have been reported: Hinrichs (1990) adjusted the position of the centre of mass (relative to segment length) from Clauser et al. (1969) and de Leva (1996) adjusted the position of the centre of mass and the radii of gyration (relative to segment length) from Zatsiorsky and Seluyanov (1983). These adjustment procedures allow the consideration of segment lengths based on joint centres instead of anatomical landmarks and were both based on mean data from six males (Chandler et al., 1975).

The current adjustment procedure allows the consideration of not only segment lengths based on joint centres, but also BSIPs directly expressed in the conventional SCSs. The segment axes follow the recommendations of the *International Society of Biomechanics* (Wu et al., 2002, 2005). The segment origin is relocated at the proximal joint centre in order to be consistent with a system of linked segments. The estimations of the *EJC*, *WJC*, *KJC* and *AJC* as well as the estimations of the distal points for the *Head & Neck*, *Hand* and *Foot* are directly based on the 3D anatomical landmarks available in McConville et al. (1980) and in Young et al. (1983). The estimations of the *CJC*, *SJC*, *LJC* and *HJC* are based on Reed et al. (1999). These estimations are preferred to other regressions (Bell et al., 1990; Davis et al., 1991; Meskers et al., 1998; Seidel et al., 1995) because they provide at the same time the *CJC* and *SJC* as well as the *LJC* and *HJC* and because they are based on the same anatomical landmarks as McConville et al. (1980) and Young et al. (1983). Additionally, these estimations distinguish between genders and deal with mean data from 33 males and 28 females for the *LJC* and *HJC* and with mean data from 25 males and 25 females for the *CJC* and *SJC*. In vivo functional estimations of the joint centres (Cappozzo, 1984; Schwartz and Rozumalski, 2005; Stokdijk et al., 2000; Veeger, 2000) should be prioritized for human movement analysis. However, if regressions are used, alternative BSIP scaling equations are provided in the current study for the *Pelvis* and *Torso*. In this way, the *Pelvis Width* and *Thorax Width* could be used for both joint centre and BSIP estimations. Also, alternative scaling equations are provided for the *Hand* and *Foot*, so that widely used segment lengths, between the *WJC* and the FT_3 and between the *CAL* and the TT_{II}, could be still considered.

The data from McConville et al. (1980) and from Young et al. (1983) were obtained by stereo-photogrammetric technique assuming constant and uniform density. This may have an influence on the BSIPs (Ackland et al.,

1988b). However, according to McConville and Clauser (1976), the position of centre of mass, the principal moments of inertia and the mass of most of the segments can be estimated from stereo-photogrammetric technique with an error of 6% (compared to direct measurements on cadavers). Additionally, compared to de Leva (1996), the current scaling equations for the segment mass, the *Y*-coordinate of the centre of mass and the moments of inertia, seem consistent for both males and females. The *Head & Neck* and *Torso* cannot be compared because of different segmentation. In addition, the present study provides scaling equations for the *X*- and *Z*-coordinates of the centre of mass and for the products of inertia. In fact, the adjusted BSIPs from McConville et al. (1980) and from Young et al. (1983) demonstrate that the centre of mass, the proximal and distal endpoints are not aligned (especially for the *Head & Neck*, *Arm*, *Hand*, *Thigh* and *Foot*) and demonstrate that the inertia tensor is not principal in the segment axes (especially for the *Torso*, *Hand*, *Pelvis* and *Foot*). The influence of these BSIP estimations on the 3D inverse dynamics should be further investigated.

The obtained scaling equations should not be used outside the population on which they are based (i.e. 30 years old males and females). Nevertheless, the studies of McConville et al. (1980) and of Young et al. (1983) also provide anthropometric measurements so that non-linear regressions as proposed by Yeadon and Morlock (1989) or Zatsiorsky and Seluyanov (1983) could be further investigated.

In closing, the current study provides, for both males and females, scaling equations for BSIPs directly applicable in conventional SCSs and without restraining the position of the centre of mass and the orientation of the principal axes of inertia. These adjusted scaling equations may be useful for researchers who would like to use appropriate 3D BSIPs for posture and movement analysis.

Acknowledgements

The authors would like to thank Frances Baxter for her critical reading of the revised manuscript.

Appendix A

Definition of anatomical landmarks from McConville et al. (1980):

Head Vertex (*HV*)	Top of the head in the mid-sagittal plane
Sellion (*SEL*)	Greatest indentation of the nasal root depression in the mid-sagittal plane
Occiput (*OCC*)	Lowest point in the mid-sagittal plane of the occiput that can be palpated among the nuchal muscles
7th Cervicale (C_7)	Superior tip of the spine of the 7th cervical vertebra
Suprasternale (*SUP*)	Lowest point in the notch in the upper edge of the breastbone
Right Acromion (*RA*)	Most lateral point on the lateral edge of the acromial process of scapula
Lateral Humeral Epicondyle (*LHE*)	Most lateral point on the lateral epicondyle of humerus
Medial Humeral Epicondyle (*MHE*)	Most medial point on the medial epicondyle of humerus
Olecranion (*OLE*)	Posterior point of olecranon
Ulnar Styloid (*US*)	Most distal point of ulna
Radial Styloid (*RS*)	Most distal point of radius
2nd Metacarpal Head (MH_2)	Lateral prominent point on the lateral surface of second metacarpal
5th Metacarpal Head (MH_5)	Medial prominent point on the medial surface of fifth metacarpal
3rd Finger Tip (FT_3)	Tip of the third finger
Midpoint between the Postero-Superior Iliac Spines (*MPSIS*)	Midpoint between the most prominent points on the posterior superior spine of right and left ilium
Right Antero-Superior Iliac Spine (*RASIS*)	Most prominent point on the anterior superior spine of right ilium
Left Antero Superior Iliac Spine (*LASIS*)	Most prominent point on the anterior superior spine of left ilium
Symphision (*SYM*)	Lowest point on the superior border of the pubic symphisis
Greater Trochanter (*GT*)	Superior point on the greater trochanter
Lateral Femoral Epicondyle (*LFE*)	Most lateral point on the lateral epicondyle of femur
Medial Femoral Epicondyle (*MFE*)	Most medial point on the medial epicondyle of femur
Tibiale Head (*TH*)	Uppermost point on the medial superior border of tibia
Fibula Head (*FH*)	Superior point of the fibula
Sphyrion (*SPH*)	Most distal point on the medial side of tibia
Lateral Malleolus (*LM*)	Lateral bony protrusion of ankle
Calcaneous (*CAL*)	Posterior point of heel
1st Metatarsal Head (MH_1)	Medial point on the head of first metatarsus
5th Metatarsal Head (MH_V)	Lateral point on the head of fifth metatarsus
2nd Toe Tip (TT_{II})	Anterior point of second toe

Appendix B

The *Lumbar Joint Centre* (*LJC*) and the *Hip Joint Centre* (*HJC*) are estimated according to Reed et al. (1999). The estimations are based on pelvis bone measurements (Reynolds et al., 1982) for midsize male (mean data from 33) and female (mean data from 28).

Flesh margin correction vectors are taken into account in order to adjust anatomical landmarks from surface to bone (Reed et al., 1999). The correction vector for both *LASIS* and *RASIS* is −10 mm on the *X*-axis. The correction vector for the *SYM* is −17.7 mm on both *X*- and *Z*-axes. The adjusted *Pelvis* ACS, computed with the corrected *LASIS*, *RASIS* and *SYM*, is consistent with Reynolds et al. (1982): the *X*-axis of the *Pelvis* ACS runs from the *RASIS* to the *LASIS*. The *Y*-axis is normal to a plane containing the *LASIS*, *RASIS* and *SYM* pointing anteriorly. The *Z*-axis is the cross product of the *X*- and *Y*-axes. The origin is the midpoint between the *LASIS* and *RASIS*.

The 3D position of the *HJC* is directly available from Reynolds et al. (1982). The 3D position of the *LJC* is extrapolated in the mid-sagittal plane by an offset vector of 10 mm perpendicular to a line connecting two available points on sacral endplate (Reed et al., 1999). The 3D positions of the *LJC* and *HJC* are scaled by the *Pelvis Width* (i.e. the distance between the *LASIS* and the *RASIS*).

For male, the *LJC* estimation is −26.4%, 0% and 12.6% of the *Pelvis Width*, respectively, on the *X*-, *Y*- and *Z*-axes. The *HJC* estimation is −20.8%, −36.1% and −27.8% of the *Pelvis Width*. For female, the *LJC* estimation is −28.9%, 0% and 17.2% of the *Pelvis Width* and the *HJC* estimation is −19.7%, −37.2% and −27.0% of the *Pelvis Width*.

Appendix C

The *Cervical Joint Centre* (*CJC*) and the *Shoulder Joint Centre* (*SJC*) are estimated according to Reed et al. (1999). The estimations are based on anthropometric measurements (Schneider et al., 1983) for midsize male (mean data from 25).

The *CJC* and *SJC* are estimated on directions orientated in the sagittal plane with respect to the vector from the C_7 to the *SUP*. The sagittal plane of the *Thorax* ACS is consistent with Schneider et al. (1983). The distances from the C_7 to the *CJC* and from the *RA* to the *SJC* are scaled by the *Thorax Width* (i.e. the distance between the C_7 and the *SUP*).

For male, the *CJC* is on a direction forming an angle of 8° with vector from the C_7 to the *SUP* and at a distance of 55% of the *Thorax Width* from the C_7. The *CJC* is positioned above the *SUP*. In a plane passing through the *RA* and parallel the sagittal plane, the *SJC* is on a direction forming an angle of 11° with vector from the C_7 to the *SUP* and at a distance of 43% of the *Thorax Width* from the *RA*. The *SJC* is positioned below the *RA*.

Based on the same anthropometric measurements (Schneider et al., 1983) for female (mean data from 25), the estimations have been completed in the current study. For female, the *CJC* is on a direction forming an angle of 14° with vector from the C_7 to the *SUP* and at a distance of 53% of the *Thorax Width* from the C_7. The *CJC* is positioned above the *SUP*. In a plane passing through the *RA* and parallel the sagittal plane, the *SJC* is on a direction forming an angle of 5° with vector from the C_7 to the *SUP* and at a distance of 53% of the *Thorax Width* from the *RA*. The *SJC* is positioned below the *RA*.

Appendix D. R_{32}

Principal radii of gyration (r_x, r_y and r_z) and elements R_{ij} of the rotation matrix of the principal axes of inertia with respect to the SCS:

		r_x	r_y	r_z	R_{11}	R_{12}	R_{13}	R_{21}	R_{22}	R_{23}	R_{31}	R_{23}	R_{33}
Head & Neck	F	32	27	33	0.9954	0.0950	0.0115	−0.0950	0.9955	−0.0018	−0.0116	0.0007	0.9999
	M	31	24	33	0.9733	0.2243	−0.0493	−0.2231	0.9743	0.0300	0.0548	−0.0182	0.9983
Torso	F	36	17	29	0.7330	−0.6782	0.0526	0.6802	0.7318	−0.0427	−0.0095	0.0671	0.9977
	M	32	18	29	0.7720	−0.6344	0.0383	0.6351	0.7724	−0.0082	−0.0244	0.0307	0.9992
Arm	F	33	15	33	0.8837	−0.0200	−0.4677	0.1176	0.9765	0.1804	0.4531	−0.2145	0.8653
	M	31	14	32	0.8992	−0.0436	0.4353	0.0376	0.9990	0.0224	−0.4353	−0.0037	0.9000
Forearm	F	27	11	26	0.8886	−0.1650	0.4281	0.2778	0.9361	−0.2159	−0.3651	0.3107	0.8776
	M	28	11	28	0.9716	−0.0150	−0.2360	−0.0090	0.9949	−0.1004	0.2364	0.0997	0.9665
Hand	F	66	35	61	0.9246	−0.3314	−0.1878	0.2185	0.8653	−0.4511	0.3120	0.3761	0.8725
	M	62	35	56	0.9631	−0.2002	−0.1798	0.1491	0.9532	−0.2631	0.2241	0.2266	0.9479

Pelvis	F	88	103	79	0.9032	−0.4293	0.0005	0.4293	0.9032	0.0003	−0.0006	−0.0001	0.9999
	M	100	107	95	0.8822	−0.4416	0.1633	0.4350	0.8972	0.0766	−0.1804	0.0034	0.9836
Thigh	F	31	19	32	0.9750	−0.0857	−0.2049	0.0660	0.9927	−0.1010	0.2121	0.0850	0.9735
	M	29	15	30	0.9850	−0.0747	−0.1554	0.0611	0.9940	−0.0908	0.1612	0.0799	0.9837
Leg	F	28	10	28	0.9611	−0.0069	−0.2762	0.0200	0.9988	0.0446	0.2755	−0.0484	0.9601
	M	28	10	28	0.9549	0.0207	0.2963	−0.0288	0.9993	0.0228	−0.2956	−0.0302	0.9548
Foot	F	17	36	35	0.9933	−0.1152	0.0101	0.1074	0.9508	0.2905	−0.0431	−0.2875	0.9568
	M	16	37	36	0.9875	0.1522	−0.0418	−0.1452	0.9798	0.1373	0.0619	−0.1295	0.9896

References

Ackland, T.R., Blanksby, B.A., Bloomfield, J., 1988a. Inertial characteristics of adolescent male body segments. Journal of Biomechanics 21, 319–327.

Ackland, T.R., Henson, P.W., Bailey, D.A., 1988b. The uniform density assumption: its effect upon the estimation of body segment inertial parameters. International Journal of Sports Biomechanics 4, 146–155.

Andrews, J.G., Mish, S.P., 1996. Methods for investigating the sensitivity of joint resultants to body segment parameter variations. Journal of Biomechanics 29, 651–654.

Apkarian, J., Naumann, S., Cairns, B., 1989. A three-dimensional kinematic and dynamic model of the lower limb. Journal of Biomechanics 22, 143–155.

Bell, A.L., Pedersen, D.R., Brand, R.A., 1990. A comparison of the accuracy of several hip center location prediction methods. Journal of Biomechanics 23, 617–621.

Cappozzo, A., 1984. Gait analysis methodology. Human Movement Science 3, 27–54.

Cappozzo, A., Catani, F., Croce, U.D., Leardini, A., 1995. Position and orientation in space of bones during movement: anatomical frame definition and determination. Clinical Biomechanics 10, 171–178.

Chaffin, D.B., Anderson, G.B.J., 1991. Occupational biomechanics. Wiley, New York.

Chandler, R.F., Clauser, C.E., McConville, J.T., Reynolds, H.M., Young, J.W., 1975. Investigation of inertial properties of the human body. Technical Report AMRL-74-137, Aerospace Medical Research Laboratory, Wright–Patterson Air Force Base, Dayton, Ohio.

Cheng, C.K., Chen, H.H., Chen, C.S., Chen, C.L., Chen, C.Y., 2000. Segment inertial properties of Chinese adults determined from magnetic resonance imaging. Clinical Biomechanics 15, 559–566.

Clauser, C.E., McConville, J.T., Young, J.W., 1969. Weight, volume, and center of mass of segments of the human body. Technical Report AMRL-TR-69-70, Aerospace Medical Research Laboratory, Wright–Patterson Air Force Base, Dayton, Ohio.

Davis, R.B.I., Õunpuu, S., Tyburski, D., Gage, J.R., 1991. A gait analysis data collection and reduction technique. Human Movement Science 10, 575–587.

de Leva, P., 1996. Adjustments to Zatsiorsky–Seluyanov's segment inertia parameters. Journal of Biomechanics 29, 1223–1230.

Dempster, W.T., 1955. Space requirements for the seated operator. WADC Technical Report TR-55-159, Wright Air Development Center, Wright–Patterson Air Force Base, Dayton, Ohio.

Doriot, N., Chèze, L., 2004. A three-dimensional kinematic and dynamic study of the lower limb during the stance phase of gait using an homogeneous matrix approach. IEEE Transactions on Biomedical Engineering 51, 21–27.

Dumas, R., Aissaoui, R., de Guise, J.A., 2004. A 3D generic inverse dynamic method using wrench notation and quaternion algebra. Computer Methods in Biomechanics and Biomedical Engineering 7, 159–166.

Dumas, R., Aissaoui, R., Mitton, D., Skalli, W., de Guise, J.A., 2005. Personalized body segment parameters from bi-planar low dose radiography. IEEE Transactions on Biomedical Engineering 52, 1756–1763.

Durkin, J.L., Dowling, J.J., 2003. Analysis of body segment parameter differences between four human populations and the estimation errors of four popular mathematical models. Journal of Biomechanical Engineering 125, 515–522.

Durkin, J.L., Dowling, J.J., Andrews, D.M., 2002. The measurement of body segment inertial parameters using dual energy X-ray absorptiometry. Journal of Biomechanics 35, 1575–1580.

Ganley, K.J., Powers, C.M., 2004. Determination of lower extremity anthropometric parameters using dual energy X-ray absorptiometry: the influence on net joint moments during gait. Clinical Biomechanics 19, 50–56.

Hinrichs, R.N., 1985. Regression equations to predict segmental moments of inertia from anthropometric measurements: an extension of the data of Chandler et al. (1975). Journal of Biomechanics 18, 621–624.

Hinrichs, R.N., 1990. Adjustments to the segment center of mass proportions of Clauser et al. (1969). Journal of Biomechanics 23, 949–951.

Jensen, R.K., 1978. Estimation of the biomechanical properties of three body types using a photogrammetric method. Journal of Biomechanics 11, 349–358.

Jensen, R.K., 1986. Body segment mass, radius and radius of gyration proportions of children. Journal of Biomechanics 19, 359–368.

Jensen, R.K., 1993. Human morphology: its role in the mechanics of movement. Journal of Biomechanics 26, 81–94.

Kadaba, M.P., Ramakrishnan, H.K., Wootten, M.E., Gainey, J., Gorton, G., Cochran, G.V., 1989. Repeatability of kinematic, kinetic, and electromyographic data in normal adult gait. Journal of Orthopaedic Research 7, 849–860.

Kingma, I., Toussaint, H.M., De Looze, M.P., Van Dieen, J.H., 1996. Segment inertial parameter evaluation in two anthropometric models by application of a dynamic linked segment model. Journal of Biomechanics 29, 693–704.

Krabbe, B., Farkas, R., Baumann, W., 1997. Influence of inertia on intersegment moments of the lower extremity joints. Journal of Biomechanics 30, 517–519.

McConville, J.T., Clauser, C.E., 1976. Anthropometric assessment of the mass distribution characteristics of the living human body. In: Proceedings of the Sixth Congress of the International Ergonomics Association, pp. 379–383.

McConville, J.T., Churchill, T.D., Kaleps, I., Clauser, C.E., Cuzzi, J., 1980. Anthropometric relationships of body and body segment moments of inertia. Technical Report AFAMRL-TR-80-119, Aerospace Medical Research Laboratory, Wright–Patterson Air Force Base, Dayton, Ohio.

Meskers, C.G., van der Helm, F.C., Rozendaal, L.A., Rozing, P.M., 1998. In vivo estimation of the glenohumeral joint rotation center from scapular bony landmarks by linear regression. Journal of Biomechanics 31, 93–96.

Mungiole, M., Martin, P.E., 1990. Estimating segment inertial properties: comparison of magnetic resonance imaging with existing methods. Journal of Biomechanics 23, 1039–1046.

Pavol, M.J., Owings, T.M., Grabiner, M.D., 2002. Body segment inertial parameter estimation for the general population of older adults. Journal of Biomechanics 35, 707–712.

Pearsall, D.J., Costigan, P.A., 1999. The effect of segment parameter error on gait analysis results. Gait & Posture 9, 173–183.

Pearsall, D.J., Reid, J.G., 1994. The study of human body segment parameters in biomechanics. An historical review and current status report. Sports Medicine 18, 126–140.

Pearsall, D.J., Reid, J.G., Ross, R., 1994. Inertial properties of the human trunk of males determined from magnetic resonance imaging. Annals of Biomedical Engineering 22, 692–706.

Pearsall, D.J., Reid, J.G., Livingston, L.A., 1996. Segmental inertial parameters of the human trunk as determined from computed tomography. Annals of Biomedical Engineering 24, 198–210.

Rao, G., Amarantini, D., Berton, E., Favier, D., 2005. Influence of body segments' parameters estimation models on inverse dynamics solutions during gait. Journal of Biomechanics, in press.

Rao, S.S., Bontrager, E.L., Gronley, J.K., Newsam, C.J., Perry, J., 1996. Three-dimensional kinematics of wheelchair propulsion. IEEE Transactions on Rehabilitation Engineering 4, 152–160.

Reed, M.P., Manary, M.A., Schneider, L.W., 1999. Methods for measuring and representing automobile occupant posture. SAE Technical Paper Series: 1999-01-0959, Society of Automobile Engineers, Warrendale, USA.

Reid, J.G., Jensen, R.K., 1990. Human body segment inertia parameters: a survey and status report. Exercise and Sport Sciences Reviews 18, 225–241.

Reynolds, H.M., Snow, C.C., Young, J.W., 1982. Spatial geometry of human pelvis. Technical Report FA-AM-82-9, FAA Civil Aeromedical Institute, Oklaoma City, Oklaoma.

Schneider, K., Zernicke, R.F., 1992. Mass, center of mass, and moment of inertia estimates for infant limb segments. Journal of Biomechanics 25, 145–148.

Schneider, L.W., Robbins, D.H., Pflug, M.A., Snyder, R.G., 1983. Anthropometry of Motor Vehicle Occupants. Volume 2: Anthropometric specifications for mid-sized male dummy. Volume 3: Anthropometric specifications for small female and large male dummies. Technical report UMTRI-83-53-2/3, University of Michigan Transportation Research Institute, Ann Arbor, Michigan.

Schwartz, M.H., Rozumalski, A., 2005. A new method for estimating joint parameters from motion data. Journal of Biomechanics 38, 107–116.

Seidel, G.K., Marchinda, D.M., Dijkers, M., Soutas-Little, R.W., 1995. Hip joint center location from palpable bony landmarks—a cadaver study. Journal of Biomechanics 28, 995–998.

Soderkvist, I., Wedin, P.A., 1993. Determining the movements of the skeleton using well-configured markers. Journal of Biomechanics 26, 1473–1477.

Stokdijk, M., Nagels, J., Rozing, P.M., 2000. The glenohumeral joint rotation centre in vivo. Journal of Biomechanics 33, 1629–1636.

Vaughan, C.L., Davis, B.L., O'Connor, J.C., 1992. Dynamics of Human Gait. Human Kinetics, Champaign, Illinois.

Veeger, H.E., 2000. The position of the rotation center of the glenohumeral joint. Journal of Biomechanics 33, 1711–1715.

Wu, G., Siegler, S., Allard, P., Kirtley, C., Leardini, A., Rosenbaum, D., Whittle, M., D'Lima, D.D., Cristofolini, L., Witte, H., Schmid, O., Stokes, I., 2002. ISB recommendation on definitions of joint coordinate system of various joints for the reporting of human joint motio—part I: ankle, hip, and spine. International Society of Biomechanics. Journal of Biomechanics 35, 543–548.

Wu, G., van der Helm, F.C., Veeger, H.E., Makhsous, M., Van Roy, P., Anglin, C., Nagels, J., Karduna, A.R., McQuade, K., Wang, X., Werner, F.W., Buchholz, B., 2005. ISB recommendation on definitions of joint coordinate systems of various joints for the reporting of human joint motion—Part II: shoulder, elbow, wrist and hand. Journal of Biomechanics 38, 981–992.

Yeadon, M.R., Morlock, M., 1989. The appropriate use of regression equations for the estimation of segmental inertia parameters. Journal of Biomechanics 22, 683–689.

Young, J.W., Chandler, R.F., Snow, C.C., Robinette, K.M., Zehner, G.F., Lofberg, M.S., 1983. Anthropometric and mass distribution characteristics of the adults female. Technical Report FA-AM-83-16, FAA Civil Aeromedical Institute, Oklaoma City, Oklaoma.

Zatsiorsky, V.M., Seluyanov, V.N., 1983. The mass and inertia characteristics of the main segments of the human body. In: Matsui, H., Kobayashi, K. (Eds.), Biomechanics VIIIB. Human Kinetics, Champaign, Illinois, pp. 1152–1159.